

Solar Zenith Angle Effects on Forest Canopy Hemispherical Reflectances Calculated with a Geometric-Optical Bidirectional Reflectance Model

Crystal Barker Schaaf, *Member, IEEE*, and Alan H. Strahler, *Member, IEEE*

Abstract—The Bidirectional Reflectance Distribution Function (BRDF) provided by the Li-Strahler geometric-optical forest canopy model has been integrated to provide spectral instantaneous hemispherical reflectances of sparsely vegetated surfaces. Further integration over the sun's zenith angles can yield daily or longer interval hemispherical reflectances as well. A variety of simulated canopies (conifer, savanna, and shrub) were modeled with varying solar angles. In all cases, as the geometric-optical model introduced increased shadowing of the surface with increased solar zenith angle, the direct-beam hemispherical surface reflectance gradually decreased. The hemispherical reflectance values are direct beam calculations and do not directly include canopy multiple scattering, leaf specularity or consideration of the impact of diffuse irradiance. These limitations are acceptable for sparse canopies, in which three-dimensional shadowing effects are large. However, radiative transfer calculations have shown that these phenomena (all of which are, to a greater or lesser extent, solar zenith-angle-dependent) must be incorporated before truly realistic modeling of hemispherical surface reflectances can be achieved for dense canopies.

Index Terms— Hemispherical reflectance, surface albedo, bidirectional reflectance distribution function, plant canopy, reflectance modeling.

I. INTRODUCTION

COMPLEX, three-dimensional surface covers such as forests and woodlands are known to exhibit highly anisotropic reflectances, due, in part, to effects such as self-shadowing and specular reflectance. This implies that spectral hemispherical reflectance, taken as the integral of the spectral BRDF over the hemisphere for a given sun position, might be quite dependent on that sun position. The Li-Strahler forest canopy model [1]–[4] accounts for the anisotropic behavior of the BRDF by using geometric optics and simple principles of Boolean set theory, and provides the opportunity to explore the diurnal variation of spectral hemispherical reflectance. The model views a sparsely covered scene as an assemblage of illuminated tree crowns of ellipsoidal shape. Under a given solar illumination angle, the areal proportions of shadowed and sunlit canopy and

of shadowed and sunlit background are determined for any viewing angle. The signatures of these areal components, as weighted by their proportions, determine the directional reflectance factor of the canopy at that viewing angle. The effects of the mutual shadowing and obscuring of tree crowns by one another are included. This reflectance model has been extended to provide instantaneous hemispherical surface reflectance computations of discontinuous vegetated canopies. Since the model produces a directional reflectance factor for each small change in viewing angle, hemispherical reflectance for a particular solar illumination angle can be calculated by the numerical integration of the directional reflectance over the viewing hemisphere. At present, this hemispherical reflectance represents a direct beam, spectrally dependent value which does not include diffuse irradiance, canopy multiple scattering, or leaf specularity effects. These deficiencies can be corrected with the introduction of more sophisticated calculations of the spectral signatures of the various components.

A. Background

Surface albedo (or hemispherical reflectance) is defined as the ratio of the total exitance reflected from a surface to the total irradiance incident on that surface within the solar (.3–4.0 μm) spectrum [5]. Exitance and irradiance measurements can be obtained in the field with downward and upward pointing full-spectrum pyranometers and used to produce instantaneous albedos. Alternatively, directional reflectance factors can be measured with narrowband radiometers at a number of view angles and then hemispherically integrated to calculate spectral hemispherical reflectances.

The majority of full spectrum albedo measurements of dense vegetation have revealed that values increase with increasing solar zenith angle [6]–[9]. This general increase in hemispherical surface reflectance, associated with increasing solar zenith angle, has also been observed in studies of broadband satellite measurements [10], although such studies use atmospherically corrected nadir reflectances as surrogate hemispherical reflectances (or albedos) and do not capture the full variability of the surface. Nunez *et al.* [11] record a similar behavior when using visible wavelength satellite measurements over Tasmania. They attribute the higher values primarily to the specular effects of the vegetation, which can be enhanced by a glancing sun angle. Some of this solar angle dependence may also be attributed to variations in the ratio

Manuscript received September 8, 1992; revised March 1, 1993. The work of the second author was supported by NASA Awards NAGW-1474 and NAS5-31369.

C. Barker Schaaf is with the Geophysics Directorate, Phillips Laboratory, Hanscom AFB, MA 01731.

A. Strahler is with the Department of Geography and the Center for Remote Sensing, Boston University, Boston, MA 02215.

IEEE Log Number 9209095.

of diffuse to direct radiation reaching the surface [12] and to the effects of multiple scattering within the canopy. Kimes and Sellers [13], on the other hand, using large numbers of field-measured directional reflectance factors to calculate spectral hemispherical reflectance in the visible band, obtain gradually decreasing spectral hemispherical reflectance values as a function of increasing solar zenith angle for such sparse cover types as orchard grass, steppe grass, and corn. The coverages in these particular cases are low and the decrease seems to be related to the shadowing of the normally bright soil backgrounds that occurs with increasing solar zenith angle.

Radiative transfer models have been used to investigate the red and near-infrared hemispherical reflectances from theoretically infinite homogeneous canopies with a variety of leaf angle distributions and leaf area indices. Kimes *et al.* [14] show that sparsely foliated homogeneous canopies produce red band hemispherical reflectances that decrease with increasing solar zenith angles. This decrease is attributed to the inability of the solar beam to penetrate the canopy at high angles and illuminate the soil background, which is bright relative to the vegetation. Dense homogeneous canopies, on the other hand, reveal a gradual increase in hemispherical reflectance with increasing solar zenith angle. In this case, very little illumination ever penetrates the dense canopy to reach the bright soil (regardless of solar zenith angle) and therefore overall hemispherical reflectance values are determined only by the dark foliage (resulting in lower values than from sparse canopies). The solar angle dependent increase is caused by the scattering properties of the upper layers of the vegetation which are emphasized at very large solar zenith angles. The near-infrared results on the other hand display increasing hemispherical reflectance with increasing solar zenith angle, regardless of canopy density. In the near-infrared, where the vegetation is bright relative to the soil, the inability, due to either high solar zenith angles or dense coverage, to penetrate the canopy and reach the soil actually enhances the hemispherical reflectance. These modeling studies are, however, for homogeneous canopies and do not take in to account any variation in tree heights and possible shadowing by nearby trees.

Otterman [15], attempts to incorporate some of this variation by modeling a canopy as a field of protrusions on a soil plane and taking the interception and projection of these protrusions into account. However, since the model uses this information to determine the penetration of the solar beam into the canopy and onto the soil, the end results are similar to those of radiative transfer models that compute the interaction of solar illumination and a turbid canopy layer.

Any such modeling studies also assume unvarying atmospheric conditions throughout a day and generate hemispherical reflectance calculations that are symmetric around the solar noon. Nkemdirim [7] reports that albedos collected with pyranometers during the morning are often less than those collected in the afternoon. Although atmospheric changes are the most likely cause of this phenomenon, the effects of leaf wilting in the warmer afternoon may also contribute. Such plant physiological changes are difficult to simulate in either geometric-optical or radiative transfer canopy models.

II. SENSITIVITY TESTS

A. Geometric-Optical Simulations

The sensitivity to solar zenith angle of the direct-beam hemispherical reflectance calculated with the Li-Strahler geometric-optical model was explored in a series of runs using realistic solar angles for the summer solstice at the latitude of Boston, MA. These systematic tests simulated several sparse, level-terrain canopies including 60% covered conifer forests (simulated as tall, thin ellipsoids, primarily 10 m wide and 20 m tall on 10 m trunks), 40% covered savanna (sparse, flat ellipsoids primarily, 10 m wide and 5 m tall on tall 10 m trunks), and 80% covered shrubland (ellipsoids sitting on the ground, primarily 0.5 m wide and 1 m tall). Since the contrast between dark canopy and bright background in red wavelength images is the reverse of that in infrared scenes (with brighter canopies and darker backgrounds), scenarios using realistic red and near-infrared areal component signatures were both evaluated (.061 for sunlit canopy, 0.15 for sunlit background, .01 for both shadowed canopy and shadowed background in the red wavelength and .55, .2, and .05 in the near-infrared).

B. BRDF's

The BRDF's of the various simulations display similar general features at any given solar angle (Fig. 1). The hotspot peak occurs when the viewing position approaches the illumination angle. Its shape is governed by the brightness contrast between tree crown and background and by the shape and density of the crowns and the rapidity with which the shadows they cast are revealed when the viewing and illumination geometry diverge. Opposite the hotspot, increasingly large areas of shadow (with lower reflectances) are viewed. An upturned bowl-shape is produced when the proportion of viewed shadows is reduced by the obscuring of the shadows by the crowns themselves (i.e., the scene brightens at the bowl edge, as only unshadowed crown tops are viewed). This mutual shadowing occurs at either high illumination or high viewing zenith angle (or both) and more so for those crown shapes (Fig. 2) that present a larger cross section at higher zenith angles (tall thinner shapes). Mutual shadowing enhances reflectance more in the near-infrared, where the unshadowed crowns reflect more brightly.

As solar illumination progresses from noon to late afternoon the position of the hotspot, of course, changes correspondingly. Beyond the hotspot region of the BRDF, larger and more elliptical shadows occur and darken the scene as the solar zenith angles increase (at least until large solar and viewing angles are reached, where the mutual shadowing effects start to occur).

C. Calculated Hemispherical Reflectances

By numerically integrating the BRDF over the viewing hemisphere, a spectral hemispherical reflectance for each solar zenith angle is obtained. The integration of each surface in Fig. 1 provides one of the data points used in the lines of conifer hemispherical reflectance shown in Fig. 3. Because the geometric-optical model produces an increasing area of shadowed surface as solar zenith angle increases, the

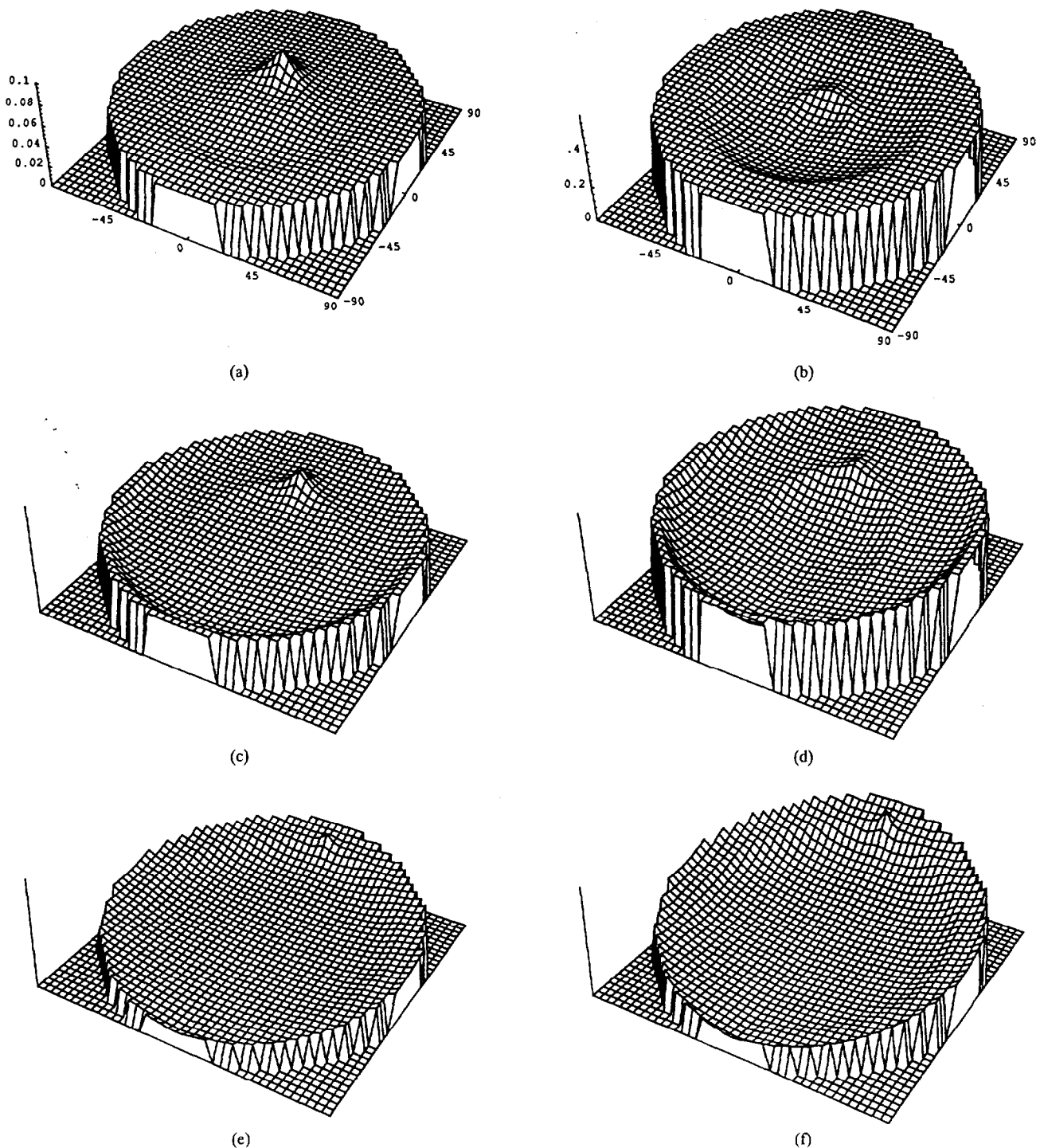


Fig. 1. The modeled BRDF of a 60% conifer covered surface in the red (a, c, e) and near-infrared wavelengths (b, d, f) for three solar zenith angles; (a, b) 18.5° , (c, d) 31.0° , and (e, f) 63.7° . Each three-dimensional BRDF is displayed in a rectangular coordinate system where each view angle in the hemisphere is taken as a pair of polar coordinates and transformed onto the x - y plane as a vector of unit length. The corresponding reflectances are then plotted along the z axis.

hemispherical reflectance obtained by integration displays a decreasing trend. This gradual decrease consistently occurs in all the simulations tested (Fig. 3). Regardless of the relative brightness or darkness of the soil and vegetation in certain wavelengths, the shadowed areas are always darker than sunlit regions and therefore any increase in shadows results in a darker scene. Since neither diffuse illumination nor multiple scattering within the canopy are accommodated in the present form of the model, these shadows remain uniformly

and unvarying dark. Although the total area of shadows may be somewhat lessened by mutual shadowing effects at very large solar zenith angles, the overall hemispherical surface reflectances do not display any major impact from this phenomenon.

A series of less populated canopies were simulated to investigate the impact of tree density. A lower coverage of trees (20% conifers, 10% savanna shapes and 30% shrubs) allows the soil background (which is illuminated at low solar

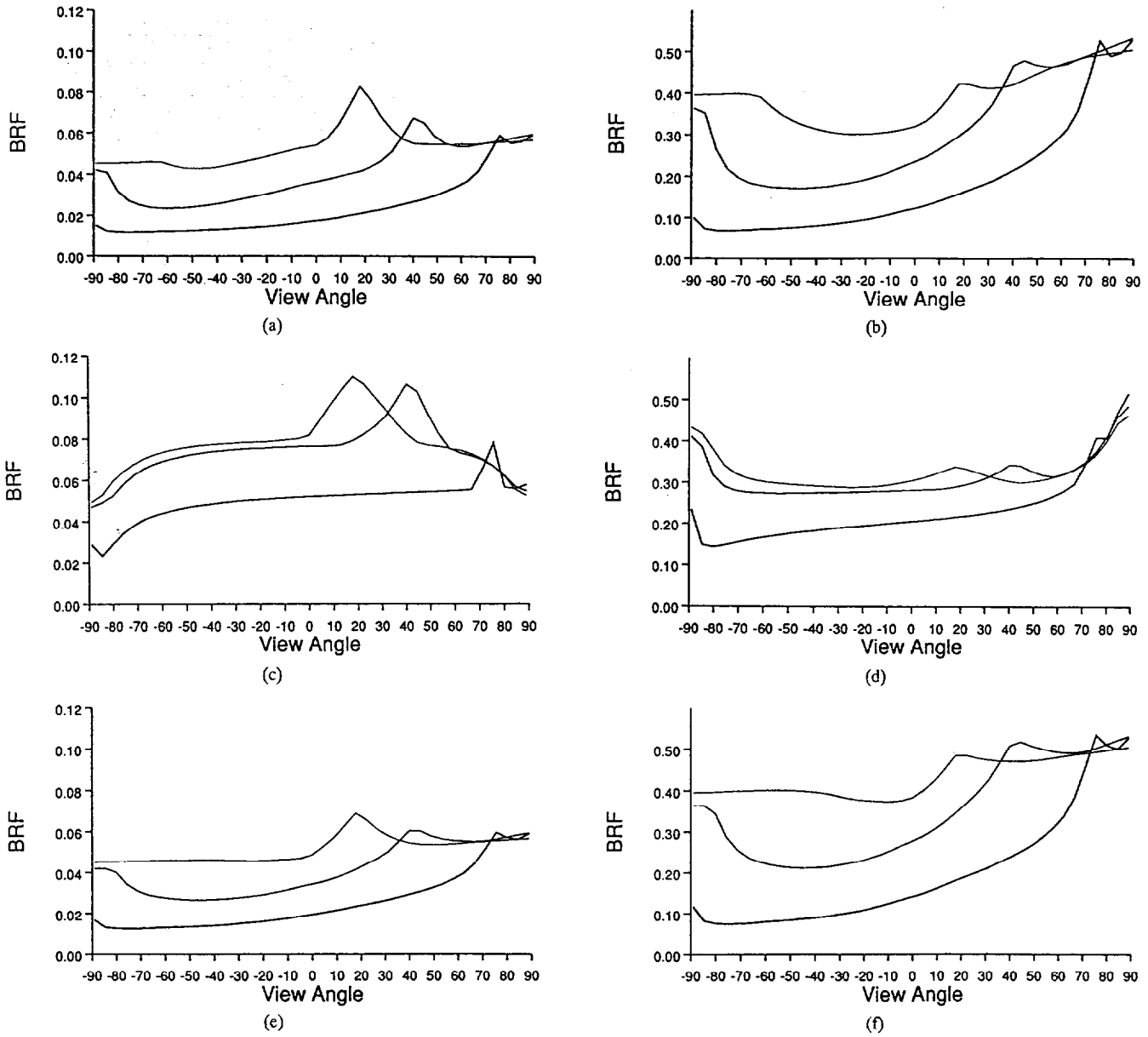


Fig. 2. The BRDF principal planes in the red (a, c, e) and near-infrared (b, d, f) wavelengths representing (a, b) 60% conifer, (c, d) 40% savanna, and (e, f) 80% shrub covered surfaces for solar zenith angles of 18.5° (—), 41.5° (---), and 74.5° (· · ·).

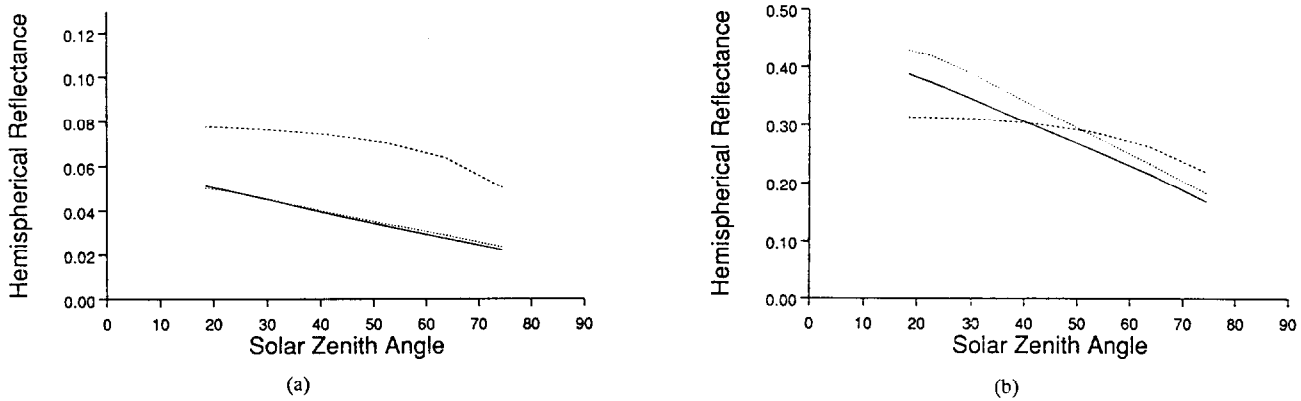


Fig. 3. The instantaneous hemispherical reflectance from the geometric-optical model for a 60% conifer (—) covered scene, a 40% savanna (---) covered scene, and a 80% shrub (· · ·) covered scene in the red (a) and near-infrared (b) wavelengths.

zenith angles) to play more of a role. The soil enhances it is illuminated and decreases them in the near-infrared the hemispherical reflectances in the red wavelengths when (Fig. 4).

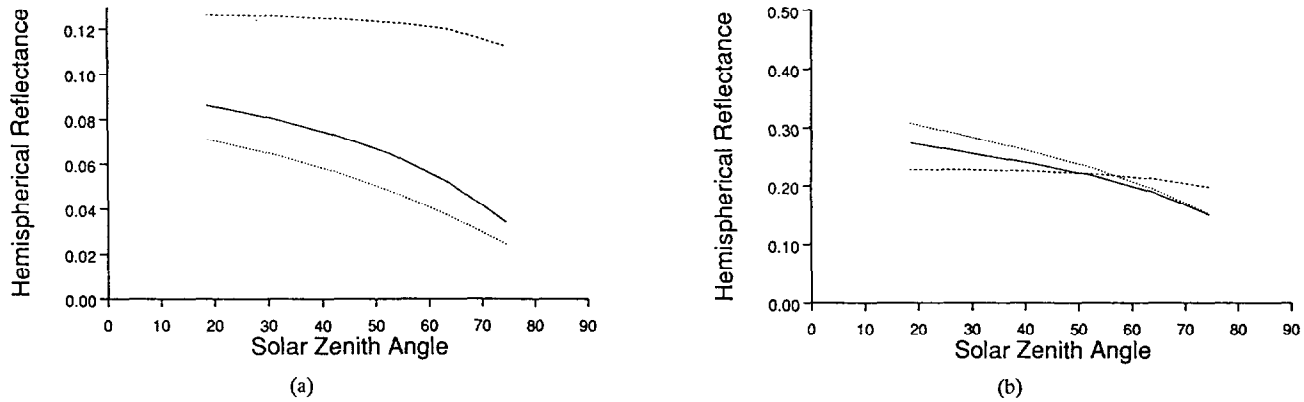


Fig. 4. The instantaneous hemispherical reflectance from the geometric-optical model for a 20% conifer (—) covered scene, a 10% savanna (---) covered scene, and a 30% shrub (···) covered scene in the red (a) and near-infrared (b) wavelengths.

As mentioned, because the Li-Strahler model utilizes component signatures, it is not directly formulated to accommodate multiple scattering within the tree canopy. Modifications to incorporate canopy multiple scattering via gap probability models [4], [16] are being explored. A multiple-scattering modification which assimilates the leaf composition of the canopy by nesting an assemblage of leaves within an envelope of a single crown is envisioned. This would solve many of the difficulties in specifying sunlit canopy component signatures *a priori*. Any such modification would also have to encompass the illumination contribution of the diffuse sky irradiance, which increases with solar zenith angle. Increased diffuse skylight will act to decrease the contrast between shadowed and sunlit areas by softly illuminating the canopy and background at angles other than just the solar direct beam geometry. Diffuse illumination will impact both the sunlit canopy component signature (by reducing the leaf shadowing occurring within a crown) and the shadowed canopy and background components (by causing some illumination to reach and lighten the large shadows cast by individual tree crowns). Furthermore, both atmospheric and canopy multiple scattering dictates that the shadows cast by a tree should not be uniformly dark but should vary, depending on the leaf density and distribution within the crown, from the center to the edges of the shadow.

Although realistic models of the shadowed components are not available, a radiative transfer model [17], which couples atmospheric calculations with a non-Lambertian canopy layer, can be used to obtain realistic sunlit canopy component signatures. The diffuse contribution to the irradiance can be modeled and its effect on a sunlit canopy component explored. Furthermore, since the radiative transfer model also includes an accommodation for leaf specularities, the specular contributions of the foliage can also be explored by inserting a reasonable leaf angle distribution. These computationally intensive radiative transfer calculations provide some insight into the amount and way the shadowed and sunlit component signatures will eventually need to be modeled to more realistically compute hemispherical surface reflectance with the simple geometric-optical model.

D. Radiative Transfer Results

The Liang-Strahler coupled radiative transfer model [17] can be used to replicate the two-stream spectral hemispherical reflectance results of Kimes *et al.* [14] (Figs. 5 and 6). In a red band ($\lambda = .65 \mu\text{m}$), a homogeneous plane-parallel canopy with an LAI of .5 results in a hemispherical reflectance that gradually decreases with solar zenith angle while a canopy with an LAI of 3 (which is dense enough foliage so that the bright soil background does not play an important role) results in one that gradually increases. In a near-infrared band ($\lambda = .8 \mu\text{m}$), where the vegetation reflects strongly, the hemispherical reflectances increase with solar zenith angle regardless of LAI. By comparing top-of-canopy hemispherical reflectances obtained with only a Rayleigh atmosphere with those computed assuming more realistic atmospheres, increased diffuse irradiance is seen to produce an increase in hemispherical reflectance that is quite uniform and only slightly solar zenith angle dependent.

By introducing a degree of specularity to the (planophile) leaf surfaces, this phenomenon can also be investigated with the radiative transfer model. The resulting specular impact is greater than that of the diffuse irradiance and more dependent on solar zenith angle (especially in the red band).

If the radiative-transfer-computed top-of-canopy hemispherical reflectances are used as appropriate sunlit canopy component signatures in the geometric-optical model, the resultant hemispherical reflectances no longer decrease as sharply with solar zenith angle (see Fig. 7 for a 60% conifer covered surface). However, since the geometric-optical model relies on areal proportions of sunlit and shadowed surfaces, and the amount of shadowed area still increases with solar zenith angle, the hemispherical reflectances persist in decreasing with solar zenith angle.

Realistic models for the shadowed components would act to lessen this decrease somewhat. Canopy multiple scattering would vary the intensity and brighten the edges of the shadowed regions. Furthermore, diffuse irradiance makes up more of the total irradiance at high solar zenith angles [12]. Therefore, although diffuse irradiance did not create a very angle-dependent impact as far as the sunlit components are concerned, it should affect the shadowed components

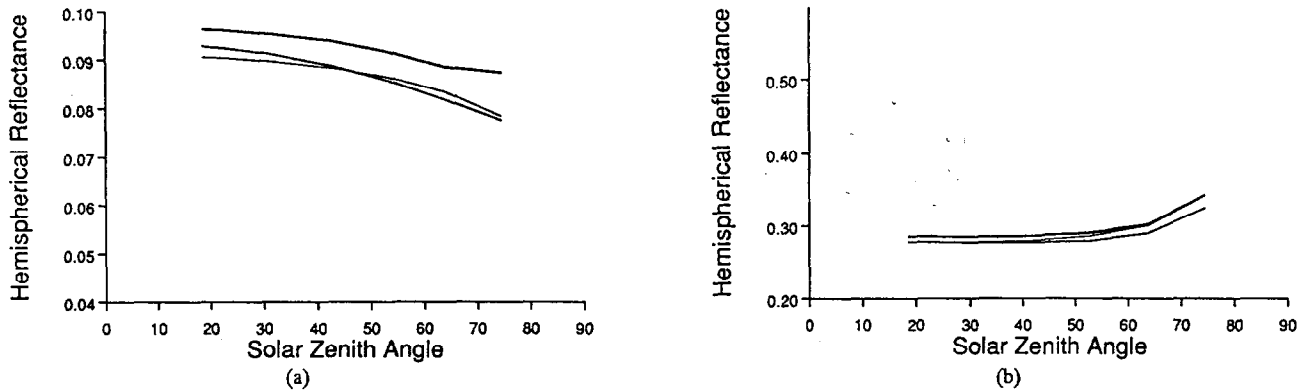


Fig. 5. Spectral hemispherical reflectances from the Liang-Strahler coupled radiative transfer model using a planophile canopy (LAI = .5) with a Rayleigh atmosphere (—), an optical depth of .1 for (a) $\lambda = .65 \mu\text{m}$ and .07 for (b) $\lambda = .8 \mu\text{m}$ (---), and the inclusion of a 1.2 specular index (-·-).

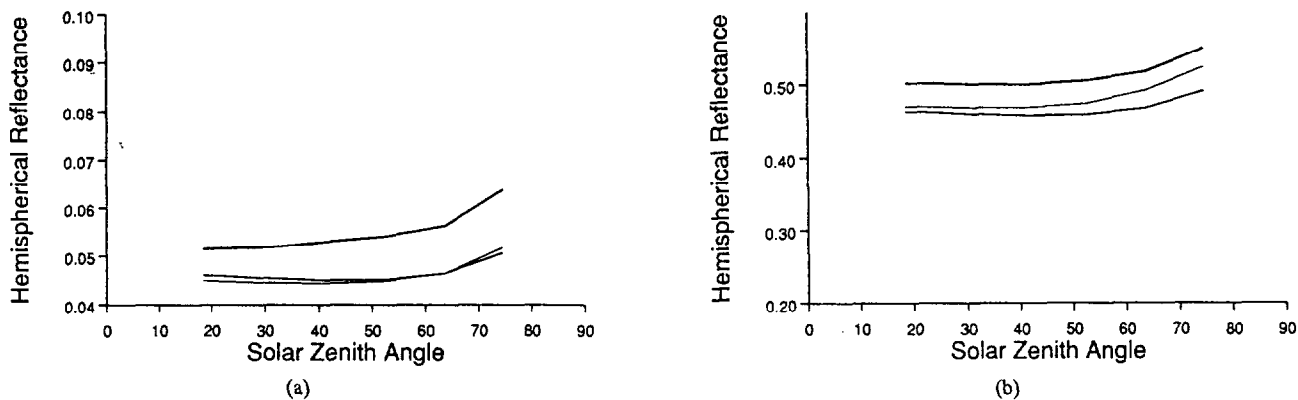


Fig. 6. Spectral hemispherical reflectances from the Liang-Strahler coupled radiative transfer model using a planophile canopy (LAI = 3) with a Rayleigh atmosphere (—), an optical depth of .1 for (a) $\lambda = .65 \mu\text{m}$ and .07 for (b) $\lambda = .8 \mu\text{m}$ (---), and the inclusion of a 1.2 specular index (-·-).

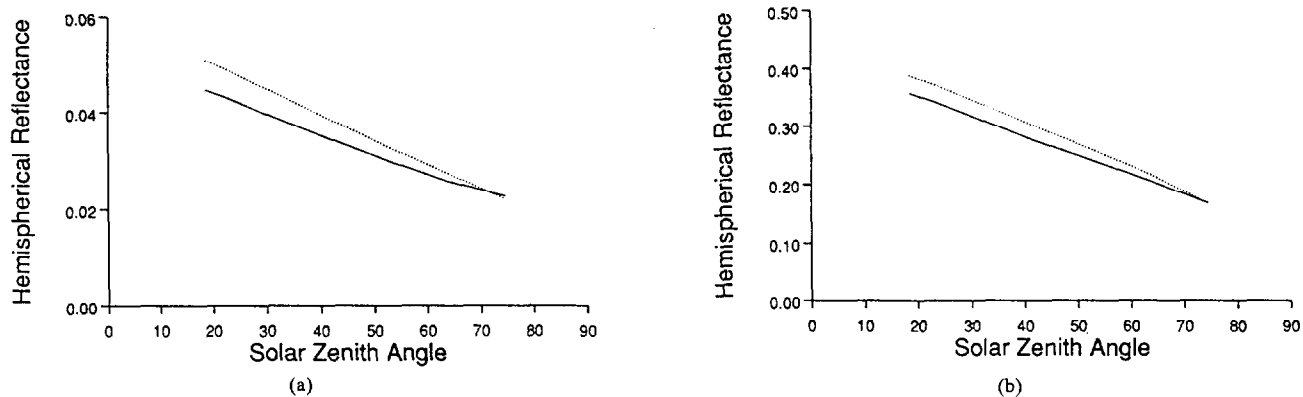


Fig. 7. Instantaneous 60% conifer covered canopy hemispherical reflectances (—) from the geometric-optical model calculated by using the dense homogeneous hemispherical reflectances from the Liang-Strahler coupled radiative transfer model as sunlit canopy component signatures (a) $\lambda = .65 \mu\text{m}$, (b) $\lambda = .8 \mu\text{m}$. The geometric-optical model hemispherical reflectances calculated with a constant sunlit canopy component signatures are provided again for comparison (···).

more significantly by lightening them as the zenith angles increase. Such shadowing models are necessary before the geometric-optical model can realistically simulate more dense canopies. Therefore although smaller total areas of shadow are computed when high tree densities and uniform heights are used, they still predominate and cause the hemispherical reflectance values of the scene to decrease with solar zenith angle. In actual forested scenes, at fairly high coverages, the canopy appears to act as a plane-parallel homogeneous layer

that is better modeled with radiative transfer codes. Currently, it is difficult to determine the density at which canopy specularly and reflectance, rather than crown shadowing, begin to play the major role. If the effect of canopy and atmospheric multiple scattering can be incorporated to reduce the impact of even small amounts of shadow at high solar zenith angles, then the signatures of the sunlit canopy component will dominate and the geometric-optical model hemispherical reflectances will approach those derived with radiative transfer codes.

III. CONCLUSIONS

Instantaneous and daily surface albedos (hemispherical reflectances) are required for surface energy budget models and local climate models. Since a forest canopy is intrinsically anisotropic, the use of a single near-nadir reflectance measurement (such as obtained from a satellite sensor) is not sufficient to estimate the instantaneous hemispherical surface reflectance. And, such measurements are rarely gathered at the full range of solar zenith angles, making daily computations difficult and forcing a reliance on modeled values. In the case of sparsely vegetated regions, the directional reflectances of a geometric-optical model can be integrated to generate direct beam hemispherical reflectances for given illumination angles, canopy characteristics, and spectral signatures. Such hemispherical reflectance calculations have been shown to have a consistent, gradually decreasing relationship with solar zenith angle, mirroring the increase in shadows cast by individual trees in a canopy.

The decreasing trend in the direct beam hemispherical reflectances can be moderated somewhat by the introduction of atmospheric and canopy multiple scattering effects, as well as the strongly solar-zenith-angle-dependent leaf specularity. By utilizing a sunlit canopy signature based on hemispherical reflectances obtained with radiative transfer calculations of a dense homogeneous canopy, some of this solar zenith angle dependence can be introduced. When the tree density is sparse, and large, clearly defined, shadowed areas appear as the solar zenith angle increases, the geometric-optical model produces realistic hemispherical reflectances (which bodes well for the use of simple models in studies of surface energy balance and ecological energetics for complex vegetation covers). However, the oversimplified handling of the shadowed regions can limit the ability of the geometric-optical model to simulate more dense uniform canopies where shadowing is less important.

ACKNOWLEDGMENT

The authors would like to thank Dr. X. Li and Dr. S. Liang for many helpful modeling suggestions and discussions.

REFERENCES

- [1] X. Li and A. H. Strahler, "Geometric-optical modeling of a conifer forest canopy," *IEEE Trans. Geosci. Remote Sensing*, vol. GE-23, pp. 705-721, 1985.
- [2] X. Li and A. H. Strahler, "Geometric-optical bidirectional reflectance modeling of a coniferous forest canopy," *IEEE Trans. Geosci. Remote Sensing*, vol. GE-24, pp. 906-919, 1986.
- [3] X. Li and A. H. Strahler, "Geometric-optical bidirectional reflectance modeling of the discrete-crown vegetation canopy: Effect of crown shape and mutual shadowing," *IEEE Trans. Geosci. Remote Sensing*, vol. 30, pp. 276-292, 1992.
- [4] A. H. Strahler and D. L. B. Jupp, "Modeling bidirectional reflectance of forests and woodlands using Boolean models and geometric optics," *Remote Sensing Environ.*, vol. 34, pp. 153-166, 1990.
- [5] F. D. Eaton and I. Dirmhirn, "Reflected irradiance indicatrices of natural surfaces and their effect on albedo," *Appl. Opt.*, vol. 7, pp. 994-1008, 1979.

- [6] J. B. Stewart, "The albedo of a pine forest," *Quart. J. Roy. Meteorol. Soc.*, vol. 97, pp. 561-564, 1971.
- [7] L. C. Nkemdirim, "A note on the albedo of surfaces," *J. Appl. Meteorol.*, vol. 11, pp. 867-874, 1972.
- [8] B. Pinty and D. Ramond, "A simple bidirectional reflectance model for terrestrial surfaces," *J. Geophys. Res.*, vol. 91-D7, pp. 7803-7808, 1986.
- [9] T. R. Oke, *Boundary Layer Climates*, 2nd ed. New York: Methuen, Inc., 1987.
- [10] H. W. Barker and J. A. Davies, "Surface albedo estimates from Nimbus-7 ERB data and a two-stream approximation of the radiative transfer equation," *J. Clim.*, vol. 2, pp. 409-418, 1989.
- [11] M. Nunez, W. J. Skirving, and N. R. Viney, "A technique for estimating regional surface albedos using geostationary satellite data," *J. Clim.*, vol. 7, pp. 1-11, 1987.
- [12] M. D. King and B. M. Herman, "Determination of the ground albedo and the index of absorption of atmospheric particulates by remote sensing. Part I: Theory," *J. Atmos. Sci.*, vol. 36, pp. 163-173, 1979.
- [13] D. S. Kimes and P. J. Sellers, "Inferring hemispherical reflectance of the earth's surface for global energy budgets from remotely sensed nadir or directional radiance values," *Remote Sensing Environ.*, vol. 18, pp. 205-223, 1985.
- [14] D. S. Kimes, P. J. Sellers, and W. W. Newcomb, "Hemispherical reflectance variations of vegetation canopies and implications for global and regional energy budget studies," *J. Clim. Appl. Meteor.*, vol. 26, pp. 959-972, 1987.
- [15] J. Otterman, "Albedo of forest modeled as a plane with dense protrusions," *J. Clim. Appl. Meteor.*, vol. 23, pp. 297-307, 1984.
- [16] X. Li and A. H. Strahler, "Modeling the gap probability of a discontinuous vegetation canopy," *IEEE Trans. Geosci. Remote Sensing*, vol. 26, pp. 161-170, 1988.
- [17] S. Liang and A. H. Strahler, "Calculation of the angular radiance distribution for a coupled system of atmosphere and canopy," *IEEE Trans. Geosci. Remote Sensing*, vol. 31, no. 2, pp. 491-502, Mar. 1993.



Crystal Barker Schaaf (M'92) received both the B.S. and M.S. degrees in meteorology from the Massachusetts Institute of Technology in 1982. She also received the M.L.A. degree in archaeology from Harvard University in 1988. She is currently a Ph.D. candidate in geography at Boston University.

She is a research meteorologist in the Satellite Branch of the Atmospheric Sciences Division, Geophysics Directorate, Phillips Laboratory, Hanscom Air Force Base, MA. Her primary research interests

are in the use of remote sensing for automated cloud analyses, the detection of initiating convective clouds, and the characterization of background surfaces, as well as the modeling of reflectances and albedo from anisotropic surfaces.



Alan H. Strahler (M'86) received the B.A. and Ph.D. degrees in geography from Johns Hopkins University in 1964 and 1969, respectively.

He is currently Professor of Geography and Researcher in the Center for Remote Sensing, Boston University, Boston, MA. He has held prior academic positions at Hunter College of the City University of New York, at the University of California, Santa Barbara, and at the University of Virginia.

Originally trained as a biogeographer, he has been actively involved in remote sensing research since 1978. He has been a Principal Investigator on numerous NASA contracts and grants, and is currently a member of the Science Team for the EOS MODIS instrument. His primary research interests are in spatial modeling and spatial statistics as they apply to remote sensing, and in geometric-optical modeling of remotely sensed scenes. He is particularly interested in remote sensing of forests and the inference of vegetation canopy parameters from digital images through invertible models.